Supplementary Material: Modelling of the COVID-19 protection framework to manage the Delta variant of SARS-CoV-2 in Aotearoa New Zealand

This appendix includes a detailed description of the model used for the B.1.617.2 (Delta) variant of SARS-CoV-2 in the New Zealand population. We model transmission of SARS-CoV-2 in the community using a stochastic age-structured branching process model (Steyn et al., 2022) in a partially vaccinated population. The model is parameterised to represent the Delta variant, which at the time the modelling was undertaken was the dominant variant globally and in New Zealand. Infected individuals are categorised as either clinical or subclinical, with the clinical fraction increasing with age. Subclinical individuals are assumed to be $\tau = 50\%$ as infectious as clinical individuals (Byambasuren et al., 2020; Davies et al., 2020). Clinical individuals are assigned a symptom onset time which is Gamma distributed from exposure time with mean 5.5 days and s.d. 2.3 days (Lauer et al., 2020). In the absence of interventions, we assume generation times follow a Weibull distribution with mean 5.05 days and s.d. 1.9 days (Ferretti et al., 2020). All parameter values used in our model can be found in Supp. Tables S1, S2 and S3.

This appendix also includes an extensive sensitivity analysis on several of the assumed model parameters. Results of the sensitivity analysis can be found in Supp. Table S6 and Supp. Figure S2.

Test-trace-isolate-quarantine system model

A test, trace, isolate, quarantine (TTIQ) system provides an additional reduction in transmission. We assume that, independently of contact tracing, the probability that an infected individual is confirmed as a case a result of symptom-triggered testing and test sensitivity is 45% for clinical individuals and 0% for subclinical individuals. There is a delay between symptom onset and detection that is assumed to be exponentially distributed with mean 4 days. We assume that the detection rate for clinical individuals is the same for vaccinated and non-vaccinated individuals and across all age groups. Once an infection is detected, the individual is assumed to be immediately isolated, resulting in an 80% transmission reduction. Some transmission may still happen within the household and isolation compliance is not perfect, hence we don't model isolation as 100% effective in reducing onward transmission. Contact tracing parameters are dependent on the number of daily cases. If the seven-day rolling average number of daily detected cases remains below 100 cases per day (contact tracing capacity) for 12 consecutive days, a proportion $p_{trace} = 0.7$ of secondary infections of a confirmed

case are identified via contact tracing and quarantined with a mean of 3 days from detection of the index case. This applies to clinical and subclinical contacts. If the number of daily detected cases exceed the contact tracing capacity, no secondary infections can be traced and quarantined (although they may still be detected as a result of symptom-triggered testing). Individuals in quarantine (i.e. asymptomatic or pre-symptomatic traced contacts) are assumed to have a 50% reduction in transmission. Individuals in isolation (i.e. confirmed cases and symptomatic traced contacts) are assumed to have an 80% reduction in transmission.

In our results, we report the percentage reduction in transmission as a result of TTIQ. We calculate this as the relative reduction in the reproduction number of individual i as a result of quarantine and isolation:

$$TTIQ_{eff,i} = 1 - \left(1 - c_{quar}\right)w_{quar,i} + (1 - c_{iso})w_{iso,i}$$

averaged over all infected individuals, where $w_{quar,i}$ and $w_{iso,i}$ are the fraction of the transmission kernel (the probability density function of the number of infection events required to link a pair of cases) that falls in the quarantine and isolation period respectively for individual i.

Age-structured transmission model

The stochastic model tracks the number of infections in the community. The population is divided into 15 five-year age bands, plus an over-75-year-old age band. The relative contact rate within each and between age groups are defined by a matrix $\hat{C}$ as in (Steyn et al., 2022). A next-generation matrix ($NGM_{i,j}$) defines the average number of individuals in group i that will be infected by a single infectious individual in group j over their whole infectious period given a fully susceptible population:

$$NGM_{i,j} = Uu_i \mathrm{M}_{\mathrm{ji}}\left[p_{clin,j} + \tau\left(1 - p_{clin,j}\right)\right]$$

where M is the contact matrix describing mixing rates between age groups (Steyn et al., 2022), u_i is the relative susceptibility to infection of age group i, $p_{clin,j}$ is the fraction of infections in age group j that are clinical, and τ is the relative infectiousness of subclinical individuals. The basic reproduction number of the age-structured model is the dominant eigenvalue of the next generation matrix, denoted $R_0 = \rho(NGM)$. In model simulations, the value of the constant U is chosen to give the desired value of R_0. We assume $R_0 = 6.0$, approximately representing the Delta variant of SARS-CoV-2 (Kang et al., 2021; Zhang et al., 2021).

The number $\lambda_{l,j}^{u}(t)$ of unvaccinated people in age group j and the number $\lambda_{l,j}^{v}(t)$ of vaccinated people in age group j who are infected by clinical individual l between time t and $t + \delta t$ are a Poisson distributed random variables with respective means:

$$\lambda_{l,j}^{u}(t) = Y_l F_l(t)\left(\int_t^{t+\delta t} w(t' - t_{inf,l})dt'\right) NGM_{j,a_l}^{clin}(1 - V_l e_T) s_j^u(t)$$
$$\lambda_{l,j}^{v}(t) = Y_l F_l(t)\left(\int_t^{t+\delta t} w(t' - t_{inf,l})dt'\right) NGM_{j,a_l}^{clin}(1 - V_l e_T)(1 - e_I) s_j^v(t) \quad (1)$$

where:

- Y_l is a gamma distributed random variable with mean 1 and variance $1/k$ representing individual heterogeneity in transmission (Lloyd-Smith et al., 2005). We set $k = 0.5$ which represents a moderate level of over-dispersion consistent with estimates for SARS-CoV-2 transmission patterns (James et al., 2021; Riou & Althaus, 2020).
- $F_l(t)$ represents the effect of quarantine or isolation on the transmission rate of individual l at time t, and is equal to 1 if individual l is not in quarantine/isolation at time t, equal to $c_{quar} = 0.5$ if individual l is in quarantine, and equal to $c_{isol} = 0.2$ if individual l is in isolation.
- $w(\tau)$ is the probability density function of the assumed generation time distribution and $t_{inf,l}$ is the time individual l was infected.
- $NGM_{j,a_l}^{clin} = Uu_j M_{a_l,j}$ is the next generation matrix for clinical individuals and a_l is the age group of individual l.
- V_l is an indicator variable that is equal to 1 is individual l is fully vaccinated at the time they became infected and 0 otherwises$_j^u(t)$ and $s_j^v(t)$ are the fractions of age group j that are unvaccinated and fully vaccinated respectively and have not previously been infected at time t.
- e_I and e_T are vaccine effectiveness against infection and against transmission given infection parameters, presented in Supplementary Table S1

The expressions for $\lambda_{l,j}(t)$ above are multiplied by τ if individual l is subclinical. Note that the factor Y_l means that, in the absence of control measures, the total number of people infected by a randomly selected individual has a negative binomial distribution with mean R_0 and variance $R_0(1 + R_0/k)$ (Lloyd-Smith et al., 2005)

At each daily time step, the susceptible compartments $s_j^u(t)$ and $s_j^v(t)$ are depleted according to the number of new infections that occurred in that compartment. Prior infection is assumed to provide complete immunity against re-infection for the duration of the simulation.

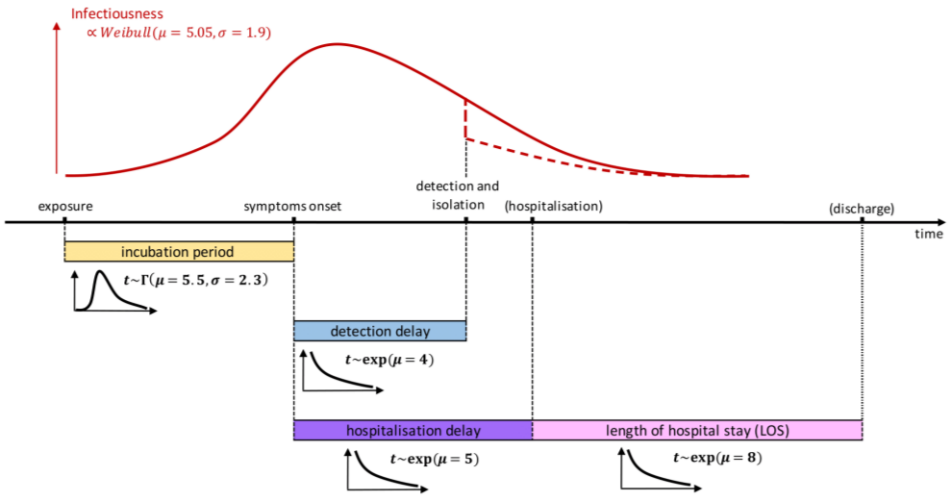

Supplementary Figure S1 Timeline showing infectiousness of a case (i.e. probability of transmitting the virus to a contact) as a function of time since infection. Infectiousness is modelled using a Weibull distribution (see Equation (1) and Supp. Table S2) with mean 5.05 days and standard deviation 1.9 days. Case detection through a positive test and isolation happen at the same time. After isolation, infectiousness is reduced to a lower level (red dashed curve, see Supp. Table S2). Subclinical infections are not isolated and follow the shape of the blue curve throughout, but with a lower overall probability of transmission. Note that this diagram does not show the possibility of quarantine through contact tracing, which would also reduce infectiousness.

Formatted: Line spacing: 1.5 lines

Formatted: Normal, Left

Hospitalisation and fatality model

Age-stratified hospitalisation rates are as in (Herrera-Esposito & de los Campos, 2021) with an additional hazard ratio of 2.26 applied to represent the increased severity of the Delta variant relative to the ancestral strain of SARS-CoV-2(Twohig et al., 2022). Fatality rates are based on those of (Herrera-Esposito & de los Campos, 2021), adjusted by an odds ratio of 2.32 for Delta (Fisman & Tuite, 2021) (Supp. Table S3). Clinical individuals in age group *i* with 2 doses of the vaccine are assumed to require hospitalisation with probability $(1 - e_D)\, p_{hosp,i}/p_{clin,i}$ where e_D is the vaccine effectiveness against severe disease in breakthrough infections (Supp. Table S1), $p_{hosp,i}$ is the infection to hospitalisation ratio for unvaccinated people in age group i (Supp. Table S3), and $p_{clin,i}$ is the fraction of infections in age group i that are clinical. The time between symptom onset and hospitalisation is assumed to be exponentially distributed with mean 5 days. The length of hospital stay is assumed to

be exponentially distributed with mean 8 days. Hospitalised cases in age group i die with probability $IFR_i/p_{hosp,i}$ where IFR_i is the infection fatality ratio for unvaccinated cases in age group *i*.

Vaccination coverage and effectiveness

Vaccine effectiveness assumptions are as shown in Supp. Table S1. All vaccinated individuals have an overall transmission reduced by $1-(1-e_I)(1-e_T)=85\%$ and an overall probability of developing severe disease reduced by $1-(1-e_I)(1-e_D)=94\%$. We use a leaky vaccine model as opposed to an all-or-nothing vaccine model, where a proportion e_I of vaccinated individuals are completely immunised and a proportion $1-e_I$ are completely susceptible (Moore et al., 2021). Reality may be somewhere between these idealised models (i.e. there may be some individual heterogeneity in the level of protection provided by the vaccine but not as extreme as all-or-nothing). The all-or-nothing and the leaky vaccine model behave similarly when the proportion of the population with immunity from prior infection is relatively small. Waning of immunity from prior infection is ignored.

Supplementary Table S1. Vaccine effectiveness parameters against Delta for the Pfizer-BioNTech vaccine after 2 doses. Source: *(Public Health England, 2021)*

Parameter	**Value**
Effectiveness against infection (e_I)	70%
Effectiveness against transmission given infection (e_T)	50%
Effectiveness against severe disease given infection (e_D)	80%
Implied overall transmission reduction	85%
Implied overall protection against severe disease	94%

Supplementary Table S2. Other parameter values used in the "baseline" scenario of our model.

Parameter	**Value**
Reproduction number excluding effects of immunity	$R_0=6.0$
Incubation period	Mean 5.5 days, s.d. 2.3 days

Generation interval	Mean 5.05 days, s.d. 1.9 days
Relative infectiousness of subclinical individuals	$\tau = 0.5$
Heterogeneity in individual reproduction number	$k = 0.5$
Probability of detection for clinical individuals	$p_{test} = 0.45$
Probability of a contact of a confirmed case being traced	$p_{trace} = 0.7$
Relative transmission rate for individuals in quarantine	$c_{quar} = 0.5$
Relative transmission rate for individuals in isolation	$c_{isol} = 0.2$
Time from symptom onset to isolation	Mean 4.0 days, s.d. 4.0 days
Time from case detection to quarantine of contacts	Mean 2.0 days, s.d. 1.2 days
Time form symptom onset to hospital admission	Mean 5.0 days, s.d. 5.0 days
Length of hospital stay	Mean 8.0 days, s.d. 8.0 days

Supplementary Table S3. Age-specific parameter values used in the "baseline" scenario of our model.

Age (yrs)	**0-4**	**5-9**	**10-14**	**15-19**	**20-24**	**25-29**	**30-34**	**35-39**	**40-44**	**45-49**	**50-54**	**55-59**	**60-64**	**65-69**	**70-74**	**75+**
2nd dose vax cov*(%)	0	0	62	88	83	84	90	91	93	90	93	92	94	95	96	96
Pr(clinical) (%)	54.4	55.5	57.7	59.9	62	64	65.9	67.7	69.5	71.2	72.7	74.2	75.5	76.8	78	80.1
Pr(hosp) (%)	0.19	0.29	0.41	0.61	0.88	1.26	1.84	2.69	3.8	5.56	8.17	11.37	16.15	22.17	30	48.97
Pr(death) (%)	8E-04	0.002	0.003	0.01	0.01	0.02	0.05	0.09	0.17	0.35	0.67	1.29	2.52	4.74	8.81	26.65
Susceptibility**	0.46	0.46	0.45	0.56	0.8	0.93	0.97	0.98	0.94	0.93	0.94	0.97	1	0.98	0.9	0.86
Popn (1000s)	306	327	335	315	337	378	380	338	311	328	329	326	295	251	217	339

* New Zealand's 1st dose vaccination coverage as of 3rd November 2021, scaled up to obtain 90% national coverage

**Susceptibility for age group i is stated relative to susceptibility for age 60-64 years (Davies et al., 2020).

Age-dependent rates of clinical disease are based on (Hinch et al., 2021).

Traffic lights trigger points

Supp. Table S4 presents the average number of hospital beds occupied when a given trigger point for the number of cases is met can be calculated as a model output, which enables the trigger points for the low, medium and high tolerance scenarios to be directly compared.

Supplementary Table S4. Trigger criteria used to raise/lower traffic light settings for low, medium, and high tolerance outbreak management responses (black text), together with the average model output number of hospital beds occupied (red text) at the time when the corresponding trigger for the number of cases was met. The high tolerance response uses hospitalisations as the trigger to move between traffic settings, whereas the other responses use reported cases. These results are provided to enable direct comparison of the criteria for moving between traffic light settings, *The "very low tolerance" triggers were only used for the border and community seed sensitivity analysis.

			Very low tolerance*	Low tolerance	Medium tolerance	High tolerance
escalation criteria	→ O	cases	10	50	200	
		hosp beds	4	20	70	100
	→ R	cases	25	100	400	
		hosp beds	9	40	140	200
	→ E	cases	50	300	1200	
		hosp beds	20	110	430	600
relaxation criteria	→ G	cases	0	0	100	
		hosp beds	0	0	40	50
	→ O	cases	10	75	300	
		hosp beds	4	30	110	150
	→ R	cases	30	200	800	
		hosp beds	10	70	290	400

Derivation of "toy border model"

Suppose there is a pre-defined tolerance y^* for prevalence $y(t)$ of active community infections. When $y(t)$ rises above y^*, stringent control measures are imposed resulting in an effective reproduction number of $R_2 < 1$. When $y(t)$ falls below some proportion α of the tolerance y^*, control measures are relaxed and the effective reproduction number is $R_1 > 1$. The parameter $\alpha < 1$ is needed to avoid instantaneous alternation between escalation and relaxation of control measures; however we will take the limit $\alpha \to 1$ to derive an idealised expression for the average proportion of time spent with control measures imposed.

In a standard SIR modelling framework, the effective reproduction number R is related to the epidemic growth rate r via

$$R = 1 + rg, \tag{2}$$

where g is the mean generation interval (Wallinga & Lipsitch, 2007).

If there are b additional infections per unit time introduced into the community via the border, then prevalence $y(t)$ is governed by the differential equation

$$\frac{dy}{dt} = ry + b. \tag{3}$$

During periods when control measures are relaxed, the prevalence at the start of the period is αy^* by definition, and subsequently grows according to

$$y(t) = (\alpha y^* + b/r_1)\, e^{r_1 t} - b/r_1 \tag{4}$$

The time taken for prevalence to rise above the threshold y^* for imposition of control measures is therefore

$$t_1 = \frac{1}{r_1} \ln\left(\frac{y^* + b/r_1}{\alpha y^* + b/r_1}\right).$$

During periods when control measures are imposed, the prevalence at the start of the period is y^* by definition, and subsequently declines according to

$$i(t) = (y^* + b/r_2)\, e^{r_2 t} - \mathrm{b/r_2}. \tag{5}$$

The time taken for prevalence to fall below the threshold αy^* for relaxation of control measures is therefore

$$t_2 = \frac{1}{r_2} \ln\left(\frac{\alpha y^* + b/r_2}{y^* + b/r_2}\right)$$

If α is close to 1, the above expressions for t_1 and t_2 may be written as a Taylor series in $1 - \alpha$:

$$t_1 = \frac{(1-\alpha)y^*}{r_1 y^* + b} + O((1-\alpha)^2), \tag{6}$$

$$t_2 = -\frac{(1-\alpha)y^*}{r_2 y^* + b} + O((1-\alpha)^2) \tag{7}$$

Over a sufficiently long time window, the approximate average proportion of time p_{int} spent with control measures in places is therefore

$$p_{int} = \frac{t_2}{t_1+t_2} = \frac{r_1+b/y^*}{r_1-r_2}, \quad (8)$$

where we have neglected terms of order $(1-\alpha)^2$ and higher.

Writing this in terms of reproduction numbers R_1 and R_2 instead of growth rates r_1 and r_2 gives

$$p_{int} = \frac{R_1-1+bg/y^*}{R_1-R_2}. \quad (9)$$

Note that for this result to be valid requires that $b < (1-R_2)y^*/g$. If $b > (1-R_2)y^*/g$, the large number of border cases means that prevalence will continue to increase above y^* even with control measures in place 100% of the time.

Converting the threshold for prevalence y^* to an approximate corresponding threshold i^* for incidence of new infections per day via $y^* = gi^*$ yields the equation in the main text for p_{int}.

Sensitivity analysis

In addition to the scenarios presented in the main text, we explore the effects of changing model assumptions for community case isolation, the probability of case detection, the effectiveness of control measures, vaccine effectiveness, the capacity of the contact tracing system, and the risk of hospitalisation (Supp. Table S5).

From each simulation, we output the number of infections, detected cases, hospital admissions and deaths, and the time spent under different traffic light settings. All simulations were run for a one year period and results were averaged over 50 independent simulations of the stochastic model for each set of parameters.

Supplementary Table S5 Parameters used in the sensitivity analysis

Parameters	Baseline values	Scenarios tested
Comm. cases isolation effectiveness (%)	100	50
Probability of case detection	0.45	0.30
Reduction in transmission (%) at G/O/R/E[1]	10/20/30/60	0/10/20/60
Vaccine effectiveness ($e_i/e_t/e_d$[2])(%)	70/50/80	50/40/80
National vaccination coverage (%)	90	95
Contact tracing	Capacity[3] = 100 cases per day pTrace[4]=70	1.No cap, pTrace=70 2.Cap=250 cases per day, pTrace=70 3.Cap=100 cases per day, pTrace=30 4.No contact tracing

[1] reduction in transmission a G/O/R/E – Green/Orange/Red and Emergency setting

[2] $e_i/e_t/e_d$ – Effectiveness of vaccine against infection/transmission given infection/disease given infection

[3] Capacity – Contact tracing capacity above which no infections are found by contact tracing compared to 70% before capacity is reached.

[4] pTrace – percentage of infections found by contact tracing before capacity is reached

Sensitivity analysis of community case isolation effectiveness

Reducing the effectiveness of case isolation in the community from 100% to 50% reduces the effectiveness of TTIQ and leads to increased transmission. As a result, the trigger points for escalating control measures are met sooner (and those for relaxing are met later), increasing the amount of time spent under more stringent settings (Supp. Fig. S2c, Supp. Table S6.C). For example, in a low tolerance

response, the time spent in the emergency setting increases from 15% to 21% (one extra month in the emergency setting) relative to the baseline scenario. The increase in time in the emergency setting is not as profound for the medium and high tolerance response. The number of infections, hospitalisations and deaths are higher than in the baseline scenario. However, this increase is offset to a large extent by the more stringent public health response described above, keeping the epidemic to pre-defined tolerances.

Sensitivity analysis of contact tracing system capacity

Under a low tolerance response, increasing contact tracing capacity from 100 cases to 250 cases per day increases the effect of TTIQ on transmission from 8% to 16%, which leads to fewer infections and hospitalisations and much less time spent in emergency setting (Supp. Table S6.G2). However, it has almost no effect on health outcomes or time spent in lockdown under a medium or high tolerance response. This is because the number of cases is almost always above 250 cases per day, so contact tracing is always performing at the reduced level in these scenarios. With no assumed limit to contact tracing capacity, there is a clear decrease in the number of infections and hospitalisations. Under a low and medium tolerance response, the time spent in red and emergency slightly increases relative to the baseline scenario as a higher proportion of infections are detected (about 50% as compared to 30% under the baseline setting) (Supp. Fig. S2g, Supp. Table S6.G1). Under a high tolerance response, the time spent in emergency decreases, but the time spent in red setting increase.

Reducing the proportion of contacts of a confirmed case who are via contact tracing from 70% to 30% has almost no effect on infections, hospitalisations or time spent in emergency setting relative to the baseline scenario (Supp. Table S6.G3) under the low and medium response. This is because the number of cases quickly exceeds the contact tracing capacity (set to 100 cases) in all scenarios. It resulted in more infections, cases, and hospitalisations, but had no effect on time spent in emergency setting under a high tolerance response.

Sensitivity analysis of probability of case detection

For the low and medium tolerance scenarios, a reduction in the probability of case detection, i.e. the probability of individuals seeking a test and testing positive, from 45% to 30% corresponds to a slower response to the increase in cases and a delayed move to higher traffic lights, leading to more infections, hospitalisations and deaths over the year (Supp. Fig. S2d, Supp. Table S6.D).

Interestingly, reducing the probability of case detection resulted in fewer infections and deaths under a high tolerance strategy than under the medium tolerance strategy. Essentially, the high tolerance strategy became more effective at controlling the spread of COVID-19 because the higher tolerance

scenario uses hospital beds as a metric of demand on the healthcare system (as opposed to case numbers in the low and medium tolerance response), which is not as affected by the lower probability of case detection. This suggests that the low and medium tolerance scenario display a higher sensitivity to the probability of case detection.

Sensitivity analysis of traffic light control effectiveness

Reducing the effectiveness of public health measures under the different traffic light settings in reducing transmission of the virus leads to a large increase in infections, hospitalisations and deaths (Supp. Fig. S2e, Supp. Table S6.E). The time spent in emergency setting is doubled under a low tolerance response (about one third of the year in emergency setting) and almost tripled under a medium and high tolerance response (2 months in emergency) relative to the baseline parameter settings.

Sensitivity analysis of vaccine effectiveness

Reducing vaccine effectiveness against infection from 70% to 50% and against transmission from 50% to 40% causes a more than a threefold increase in hospitalisations and about a twofold increase in the number of deaths (Supp. Fig. S2f, Supp. Table S6.F). The time spent in the emergency setting increases to about half of the year under a medium or high tolerance response, and about two thirds of the year under a low tolerance response.

Sensitivity analysis of vaccination coverage

Increasing the national vaccination coverage from 90% to 95% results in a significant drop in all public health outcomes and in the time spent in the red and emergency settings, with a near two-fold reduction in the number of hospitalisations and deaths (Supp. Fig. S2h, Supp. Table S6.H).

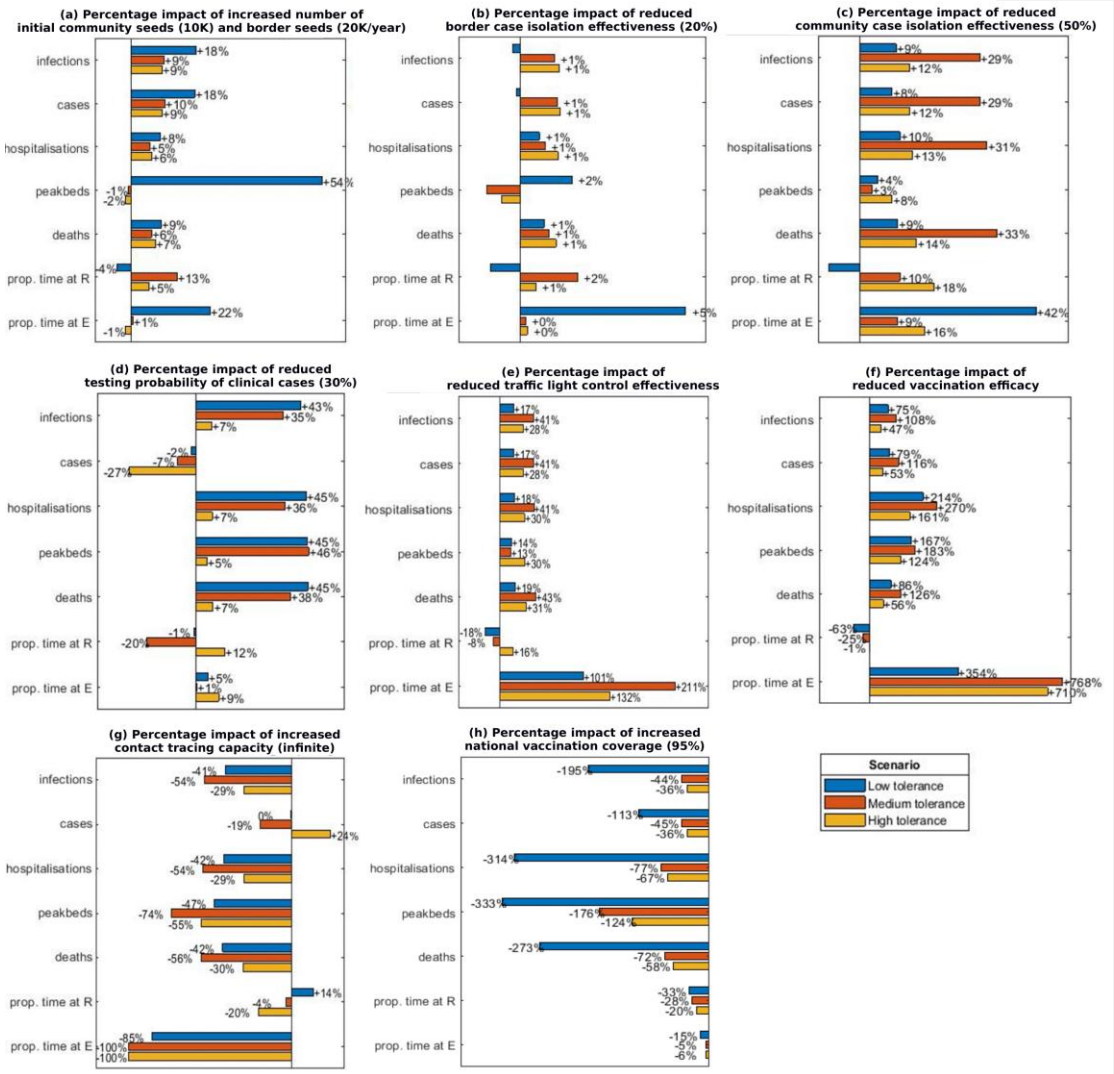

287

288 **Supplementary Figure S2** Percentage impact of different model parameter settings compared to the

289 baseline (Table 2), for the low (blue), medium (red) and high (yellow) tolerance scenarios.

290

291

292

Supplementary Table S6*:* Median number of infections, detected cases, hospitalisations, peak hospital occupancy and deaths over a year under the low, medium and high tolerance outbreak management response for all scenarios tested. The G, O, R, and E columns indicate the median percentage time spent in each of the traffic light setting (green, orange, red and emergency). The TTIQeff indicate the reduction in transmission as a result of the test, trace, isolate, quarantine system.

scenario	infections	cases	hospitalisations	peak beds	deaths	G	Y	R	E	TTIQeff
BASELINE SCENARIO										
Very low tolerance	32,000	13,000	400	40	50	0%	3%	82%	15%	12%
Low tolerance	215,000	66,000	2,900	130	410	0%	0%	85%	15%	8%
Medium tolerance	553,000	165,000	7,600	470	1,100	0%	23%	72%	5%	8%
High tolerance	684,000	204,000	9,500	650	1,390	7%	38%	49%	6%	8%
A1. Border cases = 10K										
Very low tolerance	37,000	15,000	400	40	50	0%	0%	78%	22%	12%
Low tolerance	217,000	66,000	2,900	130	400	0%	0%	84%	16%	8%
Medium tolerance	551,000	165,000	7,500	470	1,090	0%	21%	75%	5%	8%
High tolerance	690,000	206,000	9,500	650	1,390	6%	38%	50%	6%	8%
A2. Border cases = 20K										
Very low tolerance	46,000	17,000	400	40	50	0%	0%	61%	39%	11%
Low tolerance	223,000	67,000	2,800	130	400	0%	0%	84%	16%	8%
Medium tolerance	554,000	166,000	7,400	460	1,080	0%	19%	76%	5%	8%
High tolerance	703,000	210,000	9,600	650	1,410	6%	38%	50%	6%	8%
A3. Community seed cases = 10K, border cases = 10K										
Very low tolerance	93,000	32,000	1,100	200	150	0%	0%	75%	25%	10%
Low tolerance	245,000	75,000	3,200	210	450	0%	0%	82%	18%	8%
Medium tolerance	588,000	176,000	8,000	470	1,170	0%	12%	83%	5%	8%
High tolerance	725,000	217,000	9,900	640	1,460	0%	43%	51%	6%	8%
A4. Community seed cases = 10K, border cases 20K										
Very low tolerance	103,000	34,000	1,100	210	150	0%	0%	60%	40%	9%
Low tolerance	257,000	78,000	3,200	200	450	0%	0%	82%	18%	8%
Medium tolerance	604,000	181,000	8,100	470	1,170	0%	12%	83%	5%	8%
High tolerance	747,000	224,000	10,100	640	1,490	0%	44%	51%	6%	8%
B. Low border cases isolation effectiveness (20%)										
Low tolerance	216,000	66,000	2,900	130	420	0%	0%	84%	16%	8%
Medium tolerance	557,000	167,000	7,700	470	1,110	0%	20%	75%	5%	8%
High tolerance	689,000	206,000	9,600	650	1,400	6%	38%	50%	6%	8%

C. Low community cases isolation effectiveness (50%)										
Low tolerance	235,000	71,000	3,200	140	450	0%	0%	79%	21%	4%
Medium tolerance	710,000	212,000	9,900	490	1,460	0%	14%	81%	5%	4%
High tolerance	762,000	228,000	10,700	700	1,570	6%	29%	58%	7%	4%
D. Low testing probability (30%)										
Low tolerance	308,000	65,000	4,200	190	600	0%	0%	84%	16%	5%
Medium tolerance	745,000	152,000	10,400	690	1,520	2%	35%	59%	5%	5%
High tolerance	725,000	148,000	10,100	680	1,480	6%	32%	55%	7%	5%
E. Low traffic light control effectiveness										
Low tolerance	252,000	77,000	3,400	150	490	0%	0%	70%	30%	8%
Medium tolerance	774,000	231,000	10,700	540	1,570	0%	17%	67%	15%	8%
High tolerance	873,000	261,000	12,300	850	1,820	4%	25%	57%	14%	8%
F. Low vaccination effectiveness (50/40/80)										
Low tolerance	386,000	118,000	5,300	200	780	0%	0%	32%	68%	8%
Medium tolerance	1,000,000	305,000	14,100	770	2,190	0%	2%	60%	38%	8%
High tolerance	1,000,000	305,000	14,100	1,370	2,220	0%	4%	71%	25%	8%
G1. Unlimited contact tracing capacity										
Low tolerance	128,000	66,000	1,700	70	240	0%	1%	97%	2%	17%
Medium tolerance	256,000	133,000	3,500	120	490	0%	29%	71%	0%	18%
High tolerance	481,000	252,000	6,700	290	970	8%	53%	39%	0%	18%
G2. High contact tracing capacity (250)										
Low tolerance	136,000	66,000	1,800	80	250	0%	0%	97%	3%	16%
Medium tolerance	555,000	170,000	7,700	470	1,110	0%	24%	72%	5%	8%
High tolerance	679,000	206,000	9,400	650	1,380	8%	39%	48%	6%	8%
G3. Low proportion of contacts traced (30%)										
Low tolerance	219,000	66,000	2,900	130	410	0%	0%	84%	16%	8%
Medium tolerance	557,000	166,000	7,700	470	1,110	0%	20%	75%	5%	8%
High tolerance	690,000	206,000	9,600	650	1,410	6%	38%	50%	6%	8%
G4. No contact tracing										
Low tolerance	222,000	66,000	3,000	130	420	0%	0%	84%	16%	7%
Medium tolerance	558,000	166,000	7,700	470	1,100	0%	20%	76%	5%	7%
High tolerance	690,000	206,000	9,600	650	1,400	6%	38%	50%	6%	7%
H. High vaccination coverage (95%)										
Low tolerance	73,000	31,000	700	30	110	0%	48%	52%	0%	8%
Medium tolerance	383,000	114,000	4,300	170	640	9%	47%	44%	0%	8%
High tolerance	504,000	150,000	5,700	290	880	14%	57%	29%	0%	8%

298

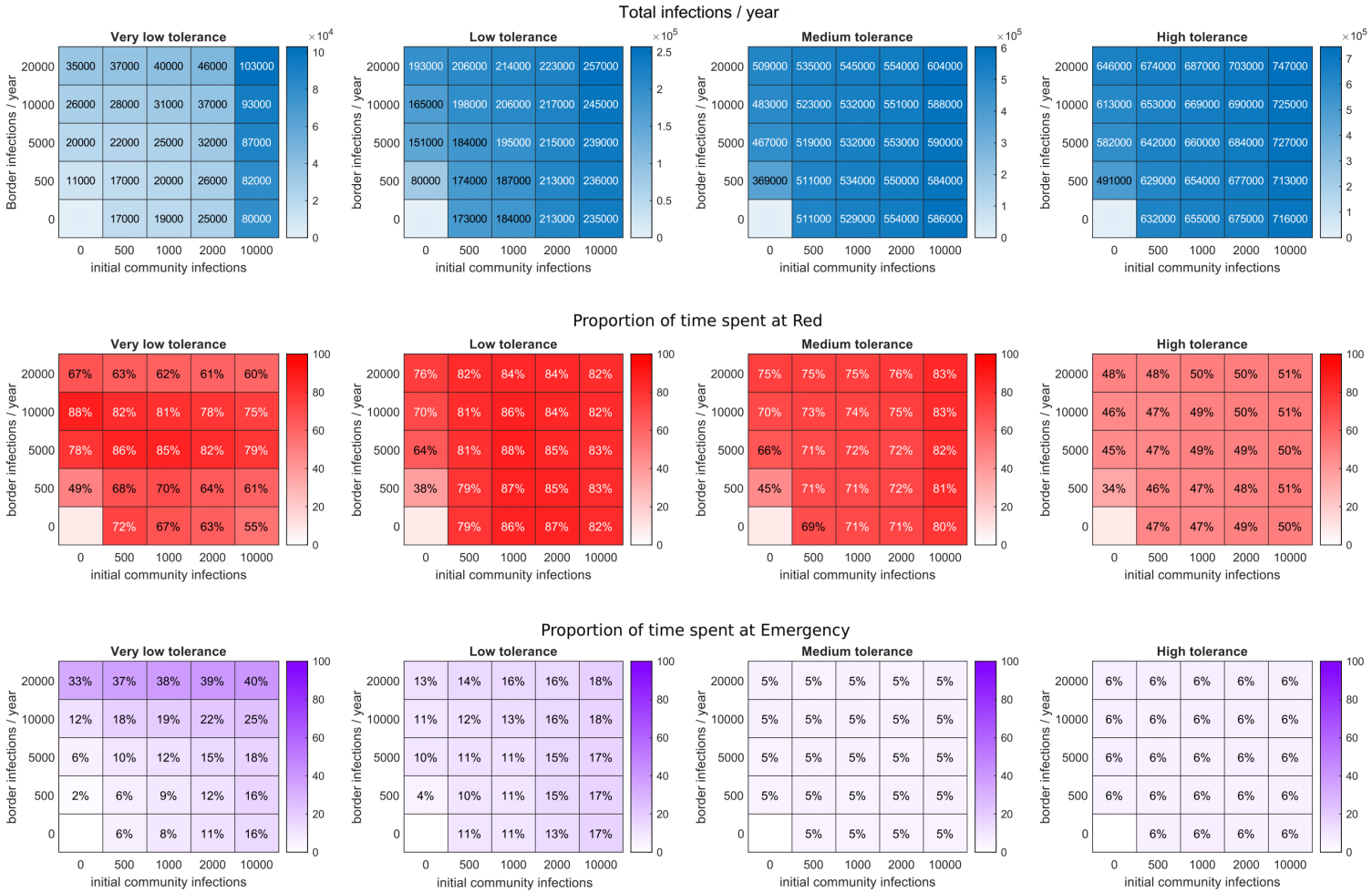

Supplementary Figure S3 Heatmaps of total infections per year (top row), proportion of time spent in the Red setting (middle row), and proportion of time spent in the Emergency setting (bottom row), for the very low (first column), low (second column), medium (third column), and high (fourth column) tolerance scenarios. Each heatmap was produced through different combinations of initial community seed infections and border infections per year, as described in Table 2.

References

Byambasuren, O., Cardona, M., Bell, K., Clark, J., McLaws, M.-L., & Glasziou, P. (2020). Estimating the extent of asymptomatic COVID-19 and its potential for community transmission: Systematic review and meta-analysis. *Official Journal of the Association of Medical Microbiology and Infectious Disease Canada*, *5*, 223–234.

Davies, N. G., Klepac, P., Liu, Y., Prem, K., Jit, M., group, C. C.-19 working, & Eggo, R. M. (2020). Age-dependent effects in the transmission and control of COVID-19 epidemics. *Nature Medicine*, *26*, 1205–1211. https://doi.org/10.1038/s41591-020-0962-9

Ferretti, L., Wymant, C., Kendall, M., Zhao, L., Nurtay, A., Abeler-Dörner, L., Parker, M., Bonsall, D., & Fraser, C. (2020). Quantifying SARS-CoV-2 transmission suggests epidemic control with digital contact tracing. *Science*, *368*(6491).

Fisman, D. N., & Tuite, A. R. (2021). Evaluation of the relative virulence of novel SARS-CoV-2 variants: a retrospective cohort study in Ontario, Canada. *CMAJ*.

Herrera-Esposito, D., & de los Campos, G. (2021). Age-specific rate of severe and critical SARS-CoV-2 infections estimated with multi-country seroprevalence studies. *MedRxiv*, https://doi.org/10.1101/2021.07.29.21261282. https://doi.org/https://doi.org/10.1101/2021.07.29.21261282

Hinch, R., Probert, W. J. M., Nurtay, A., Kendall, M., Wymant, C., Hall, M., Lythgoe, K., Bulas Cruz, A., Zhao, L., & Stewart, A. (2021). OpenABM-Covid19—An agent-based model for non-pharmaceutical interventions against COVID-19 including contact tracing. *PLoS Computational Biology*, *17*(7), e1009146.

James, A., Plank, M. J., Hendy, S., Binny, R. N., Lustig, A., & Steyn, N. (2021). Model-free estimation of COVID-19 transmission dynamics from a complete outbreak. *PLoS ONE*, *16*(3 March), 1–13. https://doi.org/10.1371/journal.pone.0238800

Kang, M., Xin, H., Yuan, J., Ali, S. T., Liang, Z., Zhang, J., Hu, T., Lau, E., Zhang, Y., & Zhang, M. (2021). Transmission dynamics and epidemiological characteristics of Delta variant infections in China. *MedRxiv*, https://doi.org/10.1101/2021.08.12.21261991. https://doi.org/https://doi.org/10.1101/2021.08.12.21261991

Lauer, S. A., Grantz, K. H., Bi, Q., Jones, F. K., Zheng, Q., Meredith, H. R., Azman, A. S., Reich, N. G., & Lessler, J. (2020). The incubation period of coronavirus disease 2019 (COVID-19) from publicly reported confirmed cases: estimation and application. *Annals of Internal Medicine*, *172*(9), 577–582.

Lloyd-Smith, J. O., Schreiber, S. J., Kopp, P. E., & Getz, W. M. (2005). Superspreading and the effect of individual variation on disease emergence. *Nature*, *438*(7066), 355–359.

Moore, S., Hill, E. M., Tildesley, M. J., Dyson, L., & Keeling, M. J. (2021). Vaccination and non-pharmaceutical interventions for COVID-19: a mathematical modelling study. *The Lancet Infectious Diseases*, *21*(6), 793–802.

Riou, J., & Althaus, C. L. (2020). Pattern of early human-to-human transmission of Wuhan 2019 novel coronavirus (2019-nCoV), December 2019 to January 2020. *Eurosurveillance*, *25*(4), 2000058.

Steyn, N., Plank, M. J., Binny, R. N., Hendy, S. C., Lustig, A., & Ridings, K. (2022). A COVID-19 vaccination model for Aotearoa New Zealand. *Scientific Reports*, *12*, 2720. https://doi.org/10.1038/s41598-022-06707-5

Twohig, K. A., Nyberg, T., Zaidi, A., Thelwall, S., Sinnathamby, M. A., Aliabadi, S., Seaman, S. R., Harris, R. J., Hope, R., & Lopez-Bernal, J. (2022). Hospital admission and emergency care attendance risk for SARS-CoV-2 delta (B. 1.617. 2) compared with alpha (B. 1.1. 7) variants of concern: a cohort study. *Lancet Infectious Diseases*, *22*, 35–42.

Wallinga, J., & Lipsitch, M. (2007). How generation intervals shape the relationship between growth rates and reproductive numbers. *Proceedings of the Royal Society B: Biological Sciences*, *274*(1609), 599–604. https://doi.org/10.1098/rspb.2006.3754

Zhang, M., Xiao, J., Deng, A., Zhang, Y., Zhuang, Y., Hu, T., Li, J., Tu, H., Li, B., & Zhou, Y. (2021). Transmission dynamics of an outbreak of the COVID-19 Delta variant B. 1.617. 2—Guangdong Province, China, May–June 2021. *China CDC Weekly*, *3*(27), 584–586.